JME

Journal of Mining & Environment,
Vol.9, No.1, 2018, 19-39.
DOI: 10.22044/jme.2017.5419.1357

Exploration of Kahang porphyry copper deposit using advanced integration of geological, remote sensing, geochemical, and magnetics data

S. Barak*, A. Bahroudi and G. Jozanikohan

School of Mining Engineering, College of Engineering, University of Tehran, Tehran, Iran

Received 16 February 2017; received in revised form 22 June 2017; accepted 5 November 2017
**Corresponding author: samaneh_barak@ut.ac.ir (S. Barak).*

Abstract

The purpose of mineral exploration is to find ore deposits. The main aim of this work is to use the fuzzy inference system to integrate the exploration layers including the geological, remote sensing, geochemical, and magnetic data. The studied area was the porphyry copper deposit of the Kahang area in the preliminary stage of exploration. Overlaying of rock units and tectonic layers were used to prepare the geological layer. ASTER images were used for the purpose of recognition of the alterations. The processes used for preparation of the alteration layer were the image-based methods including RGB, band ratio, and principal component analysis as well as the spectrum-based methods including spectral angel mapper and spectral feature fitting. In order to prepare the geochemical layer, the multivariate statistical methods such as the Pearson correlation matrix and cluster analysis were applied on the data, which showed that both copper and molybdenum were the most effective elements of mineralization. Application of the concentration-number multi-fractal modeling was used for geochemical anomaly separation, and finally, the geochemical layer was obtained by the overlaying of two prepared layers of copper and molybdenum. In order to prepare the magnetics layer, the analytical signal map of the magnetometry data was selected. Finally, the FIS integration was applied on the layers. Ultimately, the mineral potential map was obtained and compared with the 33 drilled boreholes in the studied area. The accuracy of the model was validated upon achieving the 70.6% agreement percentage between the model results and true data from the boreholes, and consequently, the appropriate areas were suggested for the subsequent drilling.

Keywords: *Fuzzy Inference System, Geographic Information System, Mineral Potential Map, Kahang, Porphyry.*

1. Introduction

The model-based mineral prospectively mapping is an approach used to minimize the size of the understudied area in mineral exploration. A mineral prospectively model is a model in which the input layers are integrated using a pre-defined function, and the result obtained is an integrated layer or mineral potential map. The input layers are the geoscience data such as the geochemical, geophysical, and geological data in the form of evidential maps. The functions used in mineral prospectively modeling is diverse in the level of model complexity. The models are classified into two types, data-driven and knowledge-driven. These models are usually conducted using the geographic information system (GIS). Many scientists such as Agterberg [1-3], Bohnam et al. [4], and Brown et al. [5] have worked on different models for the integration of geoscience layers.

Fuzzy inference system (FIS) is one of the knowledge-driven models [6]. There are three types of FISs: Mamdani style, Sugeno-style, and Tsukamoto-style. There are four inference methods of the Mamdani type including fuzzification, rule evaluation, aggregation, and defuzzification [7]. They have been successfully used in many scientific fields such as electrical and mechanical engineering, and the rest of the engineering fields or other branches of science

[8-10]. FISs of Mamdani and Tagaki-Sugeno algorithms have been used in many topics of research works in the geoscience and mining engineering. Nguyen and Ashworth have used it to develop the knowledge in the rock systems [11]. other scientists have done similar research works on the mentioned filed [12-16]. Porwal has been successfully used FIS in mineral exploration [6].

The integrated model of this research work is FIS [7]. The advantage of this integration approach is that it does not need to be trained in the same way as the advanced model of integrations such as neuro-fuzzy. Therefore, FIS can be used in any type of exploration areas as displayed by different researchers [6, 17]. The whole structure of the models in which the training data is necessary depends upon the training datasets, and they cannot be used in other cases even with similar feature conditions [17]. Any FIS model can also be updated simply by exploration miners to include new opinions and to include new variables. Since the FIS method does not need to have examples of recognized mineralization areas as the training data, it can be effectively used in the green (unknown) and brown (known) areas [6].

Pervious rock units, remote sensing, and geochemical and geophysical studies have indicated the presence of a large porphyry deposit in the Kahang area [18-21]. Initial geomagnetic magnetometry studies have been performed on the area by the Samankav Company in July 2010. The model of integration of the layers has been applied to the data for the Kahang area [18].

In this work, the mineral potential map of the Kahang area was prepared by FIS. At first, the primary layers were prepared. Right afterwards, the primary layers were integrated by Fuzzy methods, and geological, remote sensing, geochemical, and magnetics layers were prepared. These four layers were integrated using the Mamdani fuzzy inference model, and the final mineral potenatial map was created.

2. Geological settings

The Kahang porphyry copper area is located in the middle of Iran in the NE of 1:100000 Koohpayeh geological sheet in the Isfahan province. It is located between the latitudes 32° 56.7′ and 32° 55.5′ and between the longitudes 52° 26.47′ and 52° 29.9′. The understudied area is situated in the middle of Urmia-dokhtar magmatic belt, one of the Zagros main divisions [22-24]. Extension of this belt is about 2000 Km from NW to SE. Some very important porphyry copper deposits such as Sarcheshmeh, Meyduk, and Songun are placed in this belt [25]. The Kahang porphyry copper deposit is hosted by a composite intrusive comprising early diorite granodiorite and later monzonite quartz-monzonite, which was placed over a 2000 m depth, and at the temperature range of 243–600 °C [26]. The rock unit map of this area is depicted in Figure 1.

Compounds of dacite to andesitic rock involving tuffs, breccias, and lavas are the extrusive rocks in this area. The explosive eruptions of pyroclastic materials such as tuff and tuff breccia are the evidence of volcanic events in the Kahang area. Subsequently, the establishment of sub-volcanic and intrusive rocks with andesitic, dicitic, dioritic, and monzonitic occurred [26]. NW to SE is the main trend of faults as depicted with Rose diagram in Figure 2 (modified by the National Copper Company in Iran [27]).

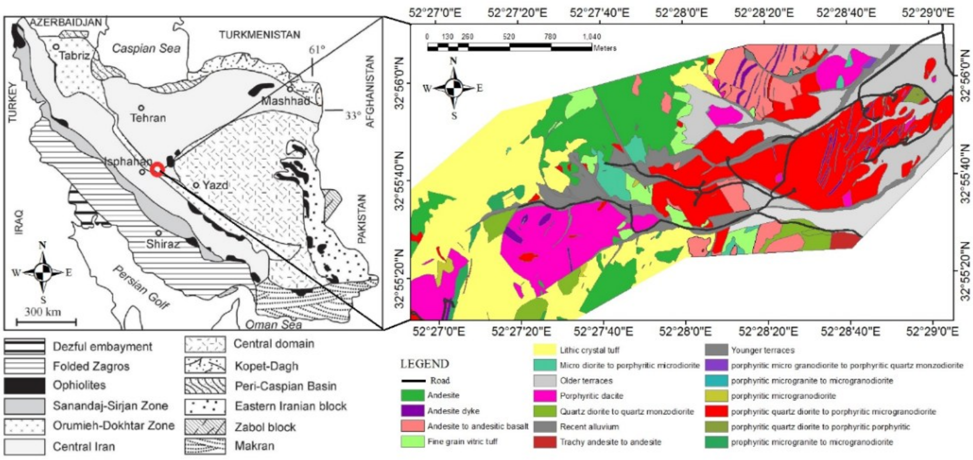

Figure 1. Modified geological map of Kahang, scale: 1.10,000, within Urumieh–Dokhtar volcanic belt in structural map of Iran [22].

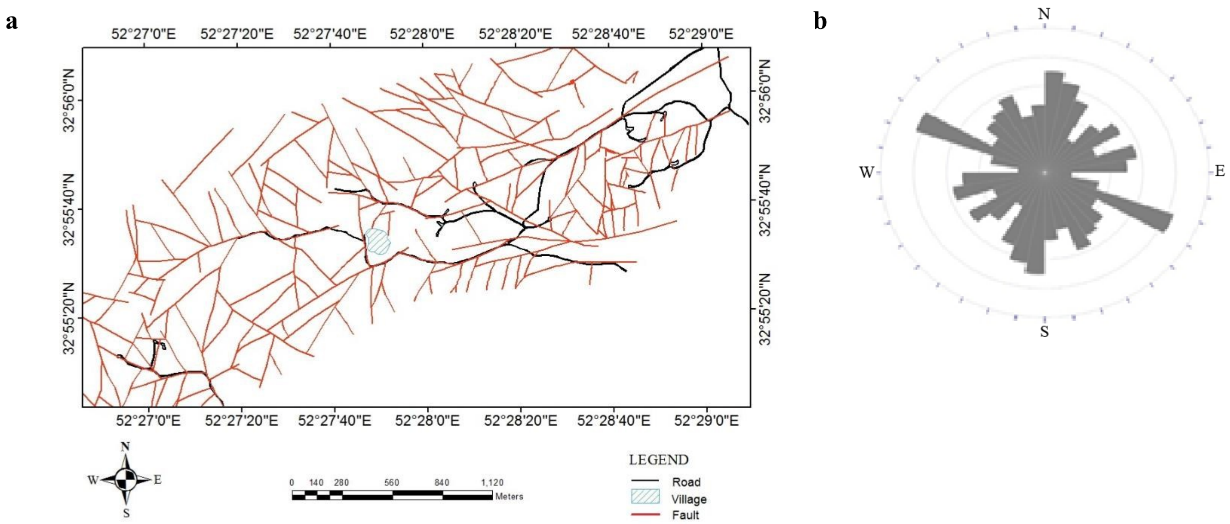

Figure 2. (a) Fault map of Kahang area (b) Rose diagram showing faults in studied area (modified by National Copper Company in Iran [27]).

3. Preparation of geological layer

In order to prepare the geological layer, rock units and tectonic layers must be created. At first, the tectonic layer was created in order to create the tectonic layer, and the fault and fault intersection layers were integrated by gamma = 0.9, as shown in the algorithm of Figure 3a. These faults were studied, and the values obtained were assigned to three models including buffering, density of the faults, and importance of the faults by azimuth.

According to the previous studies in central Iran and territories around the area, the importance of relation between azimuth of fault structures and trend of mineralization are known. In the following, the intersection of faults was studied and the values were assigned in three models including buffers, density of the fault intersection, and importance of the fault intersection by azimuth of the faults [28]. More details are given in the Table. 1.

In order to prepare the rock unit layer, rock units of the same grade of importance were used in the same groups. The importance of host rocks in the porphyry copper deposits was considered in the stage of assigning values to the rock units. Important units including granodiorite and monzonite gained the most values (Figure 3b). Details of the value assignments are displayed in Table 1.

Finally, to prepare the geological layer, rock units and tectonic layers were overlaid by gamma = 0.85, and the final geological layer was created and depicted in Figure 3c.

4. Preparation of remote sensing layer

In order to prepare the remote sensing layer, the data from the remote sensing and geological studies were used. Having done the geometric and radiometric corrections on the ASTER data, bands numbers 1 to 9 of remote sensing images were selected to be used in the remote sensing layer. Here, the image-based (RGB, band ratio and principal component analysis) and the spectrum-based (spectral angel mapper and spectral feature fitting) methods were applied on the images.

Analysis of the satellite images to extract information by combination of bands in the state of one band is defined by the false color composite. This combination is beneficial to validate alternations [29, 30]. In order to detect the argyllic alternation, RGB(468) was used (Figure 5a). Band ratioing is a very simple and powerful method in remote sensing. The basic idea of this method is to accentuate or exaggerate the anomaly of the target object [31]. Band ratio reduces the effect of topography, and therefore, augmentation of the differences between the spectral responses of each band [32]. In this work, the sericite, kaolinite, and Chlorite minerals were the key targets to find out any alteration zone. Sericite was used to validate the phyllic alternation by the ratio represented in Table 2; the resulting map is shown in Figure 5c.

The main aim of using a principal component analysis (PCA) is to reduce the dimensions of the data, here, the number of original bands, and to maximize the amount of information from the original bands into the least number of principal components. The original bands are transformed into the principal components, which contain the maximum original information with a physical meaning that is required to be explored [33]. Due to the absorption and reflection bands of sericite, the 4, 6, and 7 bands were used to validate the phyllic alternation in the Kahang area by a mini-table that is represented in Table 2 (Figure 5e).

The Spectral Angel Mapper (SAM) is one of the leading classification approaches because it estimates the spectral similarity to suppress the influence of shading to emphasize the purpose reflectance characteristics [34, 35]. In this method, the grade of similarity between two spectra is measured by the angle between spectrals [36]. Generally, the basis of the spectrum-based methods is the comparison of the reference spectrum and the spectrum of mineral, if both spectra are similar; this means that the mineral we are looking for has been validated in the area. The reference spectra that are used to validate the alternation zones are shown in Figure 4. These spectra can be obtained from the spectral library. SAM is a controlled classification method. In order to identify the phyllic alteration by the SAM method, the reference spectrum of sericite was used. The optimum angle for the phyllic alteration was 0.19 (Figure 5h). For each alternation, different angles were selected, and according to the results obtained, the optimum angle was selected.

Spectral Feature Fitting (SFF) is a commonly utilized method for hyper-spectral imagery analysis to discriminate ground targets. Compared to the other image analysis methods, SFF does not assure a higher precision in extractive image information in all status [37]. SFF is an absorption-feature-based methodology. The reference spectra are scaled to match the image spectra after the continuum is removed from both datasets [38]. In order to identify the propylitic alteration by the SFF method, the reference spectra of chlorite, epidote, and calcite were used. After processing the reference spectrum of chlorite with the aster image of the area, the results obtained showed the similarities between the spectra of the selected pixels (Figure 5k) and the reference spectrum. The details of the methods for other alternations are shown in Table 2.

In the final remote sensing layer, both the phyllic and argyllic alterations are the results of image-based and spectrum-based methods, while the propylitic alteration is the result of the spectrum-based methods. The basis of these selections are the compliance of the zones with rock units and the results provided from the RGB images. The Potassic zones shown in Figure 5n are the results of geology studies carried out by the National Copper Company in Iran [27]. In the stage of assigning values to the alteration zones, the conceptual models of porphyry copper deposits were used according to these types of deposits potassic zones including the most amount of copper, so it gains the most value of weight. The details of the value assignments are displayed in Table 1. The fuzzified remote sensing layer is shown in Figure 5o.

5. Preparation of geochemical layer

Since the Kahang area is hot and dry, the residual soil samples were used as the geochemical data. The total number of samples were 2564 (Figure 6). The soil samples weighting approximately 300 g were sampled and analyzed for 42 elements using an ICP-MS machine. The location of each sample was indicated in Figure 6. The size distribution varied from 250 to 400 micrometers. ICP-MS results for the elements are provided in Table 3.

At first, the descriptive statistics applied on data is shown in Table 3. Afterwards, all data went through the pre-statistical data processing methods such as detection of censored data and replacing, correcting the out-of-order values, and normalization. Finally, multivariate statistical processing was applied on the data. The Pearson correlation matrix and cluster analysis were used as multivariate statistical approaches. The strongest correlation coefficient between copper and molybdenum was achieved to be 0.334. The cluster analysis also showed that the two elements copper and molybdenum were in one sub-branch (Figure 7).

Application of concentration-number (C-N) multi-fractal modeling was used for the geochemical anomaly separation in both the copper (Figure 8a,c) and molybdenum (Figure 8b,d) layers. In the stage of assigning values to the zones of the geochemical layer, the probable anomaly gained the most value because of its nature; the mentioned zone had the most amount of copper or molybdenum in deposits; details of the value assignments are displayed in Table 1. Both the fuzzified copper and fuzzified molybdenum layers are shown in Figure 8e,f. The final geochemical layer was obtained by integrating the two layers (copper and molybdenum) with 'OR' fuzzy function.

Table 1. Weights assigned to factor layers in Kahang area.

Layer	Class	Allocated weight
Faults		
Azimuth with 40 m buffering	Azimuth 0° to 10° (A)	7
	Azimuth 10° to 60° (B)	9
	Azimuth 60° to 80° (C)	6
	Azimuth 80° to 130° (D)	4
	Azimuth 130° to 150° (E)	3
	Azimuth 150° to 180° (F)	2
40 m buffering	5 m	9
	10 m	7
	20 m	4
	30 m	3
	40 m	2
Fault intersection		
importance of faultsintersection by azimuth of faults	A-B, B-B	9
	B-C, B-D, B-E, B-F	8
	Intersection of A and C with each of D, E, and F	5
	Intersection D, E, and F with each other	4
40 meters buffering	8 m	9
	16 m	8
	24 m	6
	32 m	3
	40 m	2
Rock units		
	Granodiorite & Monzodiorite	9
	Andesite	7
	Tuff	6
	Dacite	5
	Andesitic dyke	2
	Alluvium	1
Magnetics		
(Analytical signal map)	High	9
	Medium	7
	Low	4
	Very low	2
	Background	1
Geochemistry		
Cu	Probable anomaly	9
	Possible anomaly	7
	Threshold	4
	Background	1
Mo	Probable anomaly	8
	Possible anomaly	6
	Threshold	2
	Background	1
Remote sensing		
	Potassic	9
	Phyllic	8
	Argillic	7
	Propylitic	3

a

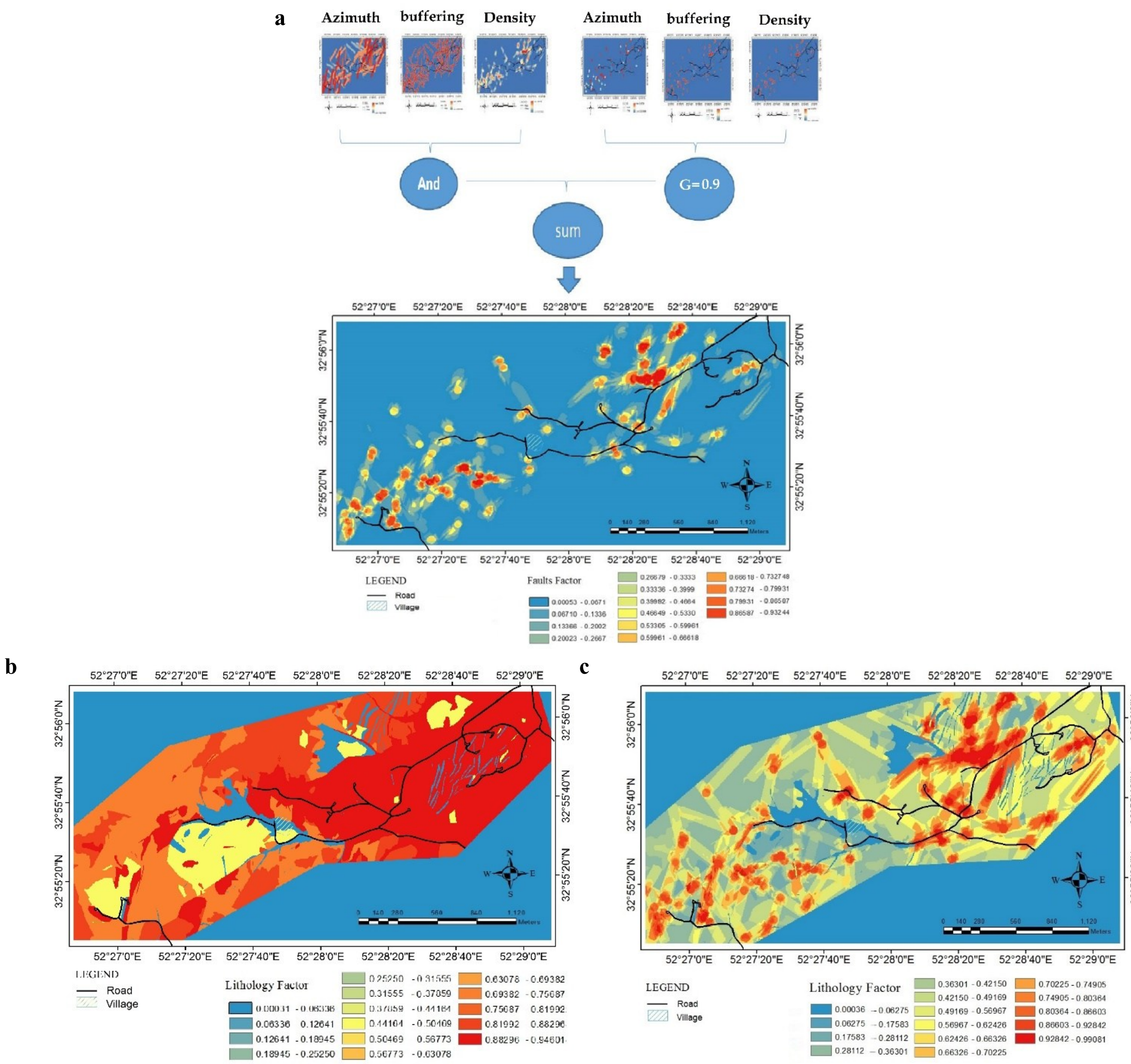

Figure 3. (a) Fault factor map and (b) rock units' factor map for understudied area, (c) final geological factor map for Kahang area.

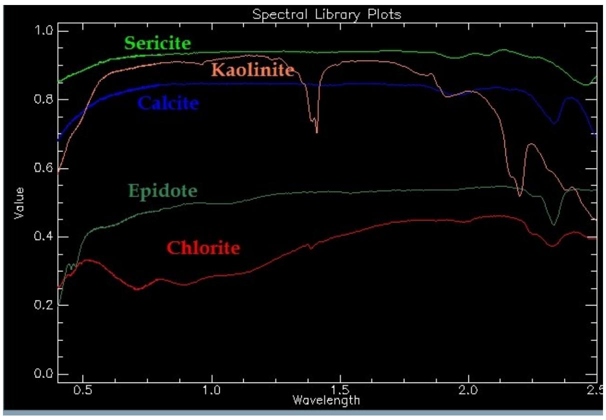

Figure 4. Reference spectrum used for detecting alternation by spectrum-based methods.

Table 2. Process of remote sensing in understudied area.

Image-based

Method	Alternation	False color composite	Figure	Color of alternation area in map
RGB	Phyllic	RGB(468)	(Figure 5a)	Brown
	Argyllic	RGB(468)	(Figure 5a)	Orange
	Propylitic	RGB(468)	(Figure 5a)	Light green

Method	Alternation	Mineral used	Band ratio	Figure	Color of alternation area in map
Band Ratio	Phyllic	Sericite	$\frac{\text{Band 4 + Band 7}}{\text{Band 6}}$	(Figure 5b)	Pink
	Argyllic	Kaolinite	$\frac{\text{Band 4 + Band 6}}{\text{Band 5}}$	(Figure 5c)	Purple
	Propylitic	Chlorite	$\frac{\text{Band 7 + Band 9}}{\text{Band 8}}$	(Figure 5d)	Blue

Method	Alternation	Used mineral and bands	PCA (Eigenvector)					Figure	Color of alternation area in map
PCA	Phyllic	Bands 4, 6, and 7 of sericite	Phyllic	Band 4	Band 6	Band 7		(Figure 5e)	Crimson
			Pc1	0.6141	0.5658	0.5501			
			Pc2	0.7849	-0.3658	-0.4999			
			Pc3	0.0816	-0.7389	0.6688			
	Argyllic	Bands 4, 5, and 7 of Kaolinite	Argyllic	Band 4	Band 5	Band 7		(Figure 5f)	Purple
			Pc1	-0.6250	-0.5578	-0.5459			
			Pc2	-0.7595	0.2743	0.5859			
			Pc3	0.1791	-0.7832	0.5952			
	Propylitic	Bands 1, 6, 7, and 9 of Chlorite	Propelytic	Band 1	Band 6	Band 7	Band 9	(Figure 5g)	Green
			Pc1	0.3995	0.5515	0.5377	0.4969		
			Pc2	0.9156	-0.2778	-0.2204	0.1893		
			Pc3	0.0196	0.4948	-0.8106	0.3123		
			Pc4	-0.0397	-0.6113	-0.0707	0.7871		

Spectrum-based

Method	Alternation	Spectrum of mineral	Optimum angle	Figure	Color of alternation area in map
SAM	Phyllic	Sericite	0.19	(Figure 5h)	Red
	Argyllic	Kaolinite	0.17	(Figure 5i)	Pink
	Propylitic	Chlorite	0.5	(Figure 5j)	Green

Method	Alternation	Spectrum of mineral	Figure	Color of mineral area in map
SFF	Propylitic	Chlorite	(Figure 5k)	Purple pixels are similar to reference spectrum
		Epidote	(Figure 5l)	Yellow pixels are similar to reference spectrum
		Calcite	(Figure 5m)	Green pixels are similar to reference spectrum

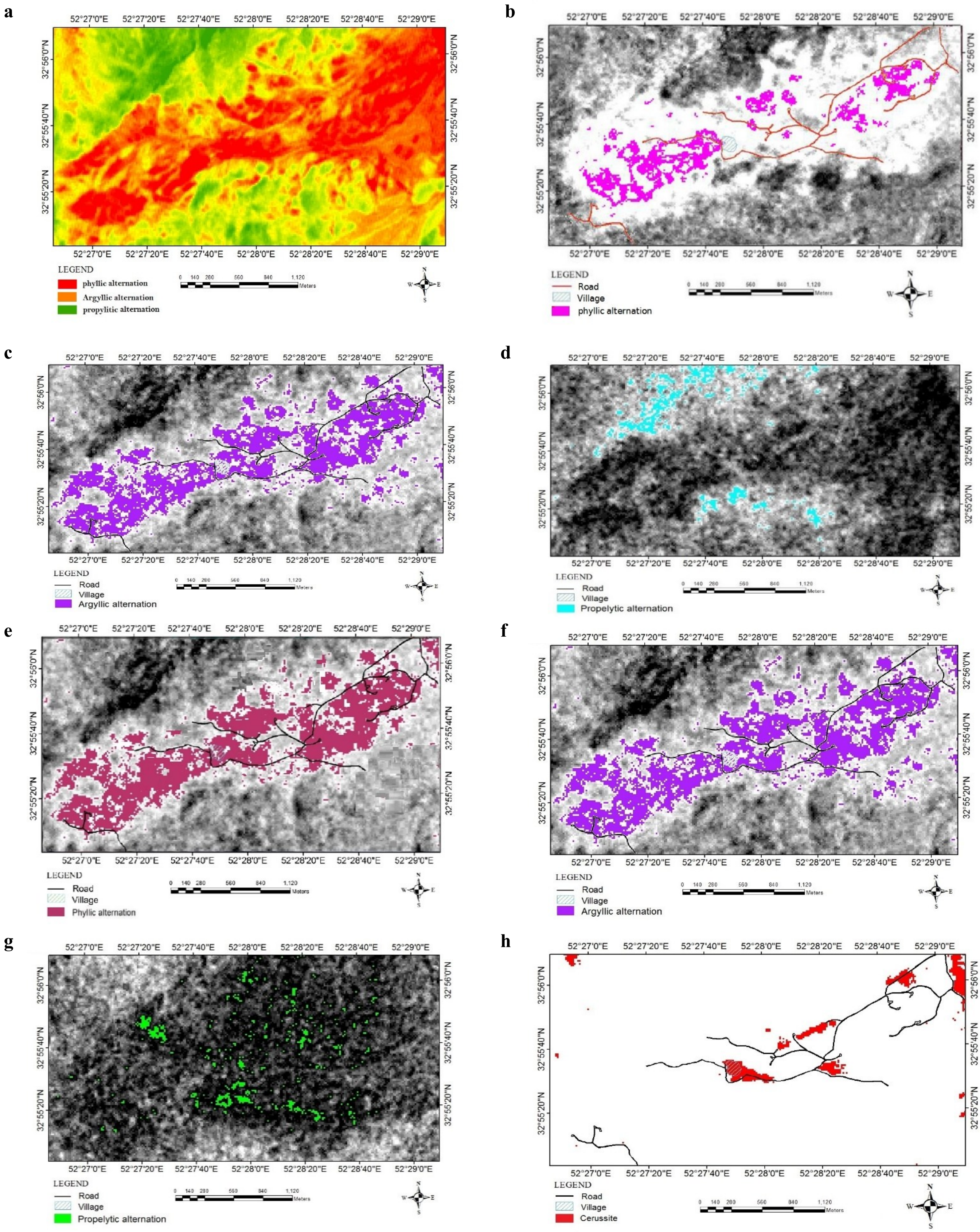

Figure 5. (a) to (m) Output of remote sensing methods, (n) final remote sensing factor map, (o) final remote sensing fuzzy map of Kahang area.

i

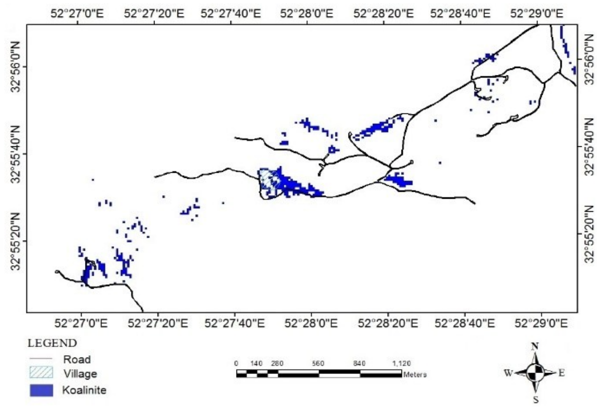

j

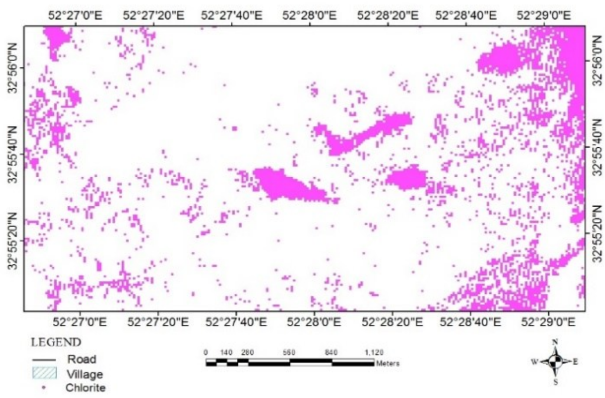

k

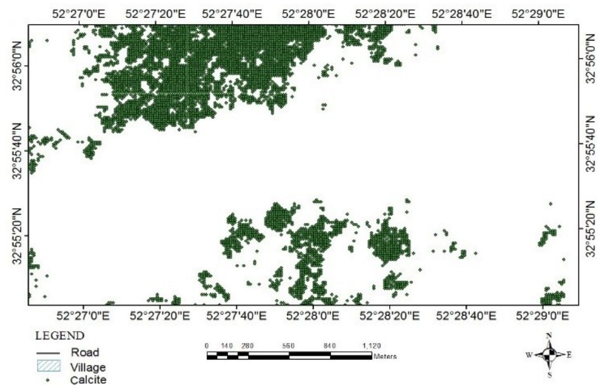

l

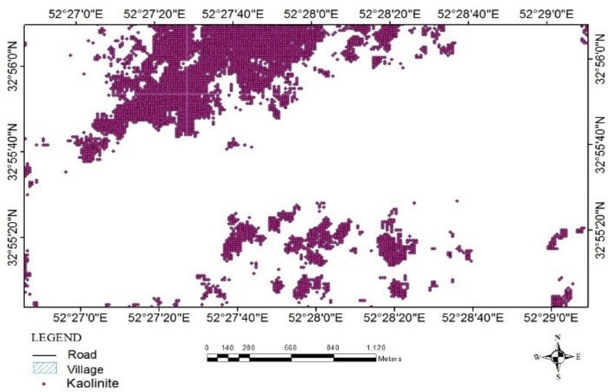

m

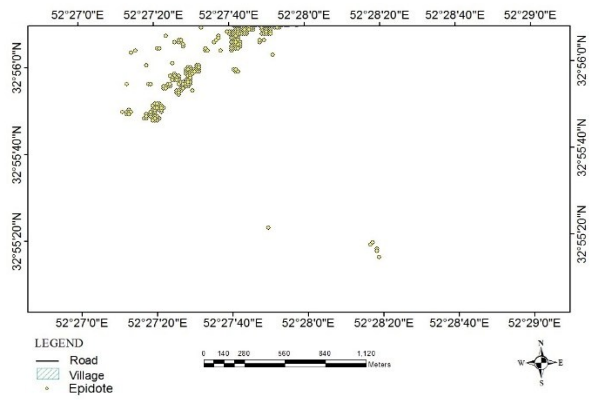

n

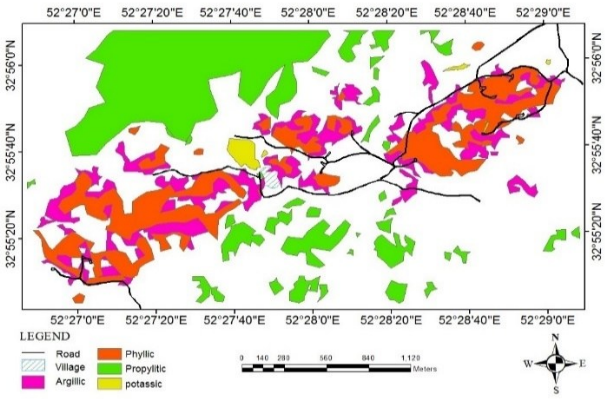

o

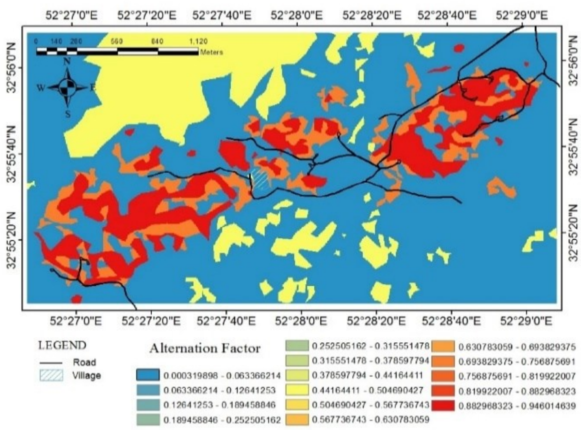

Figure 5. Continued.

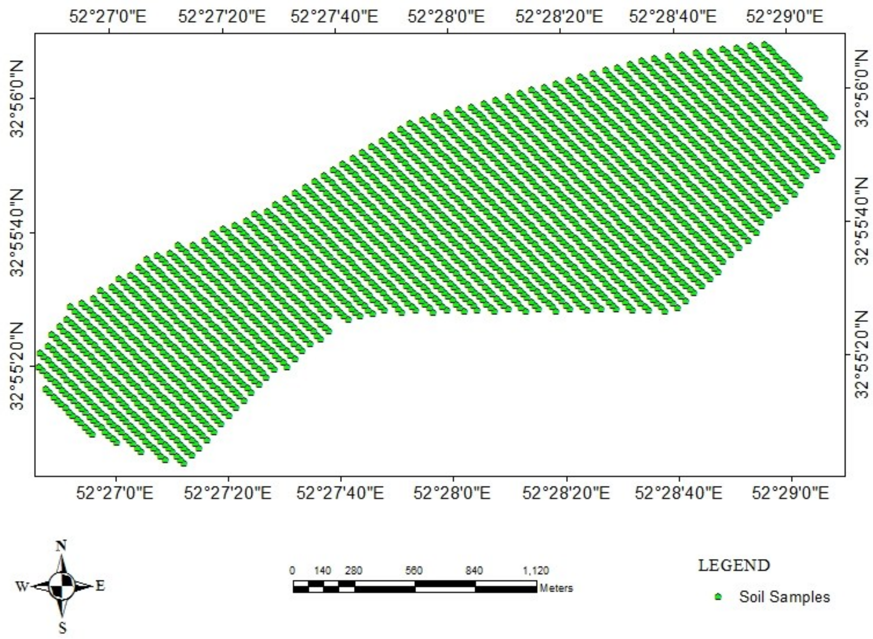

Figure 6. Sampled locations in Kahang area.

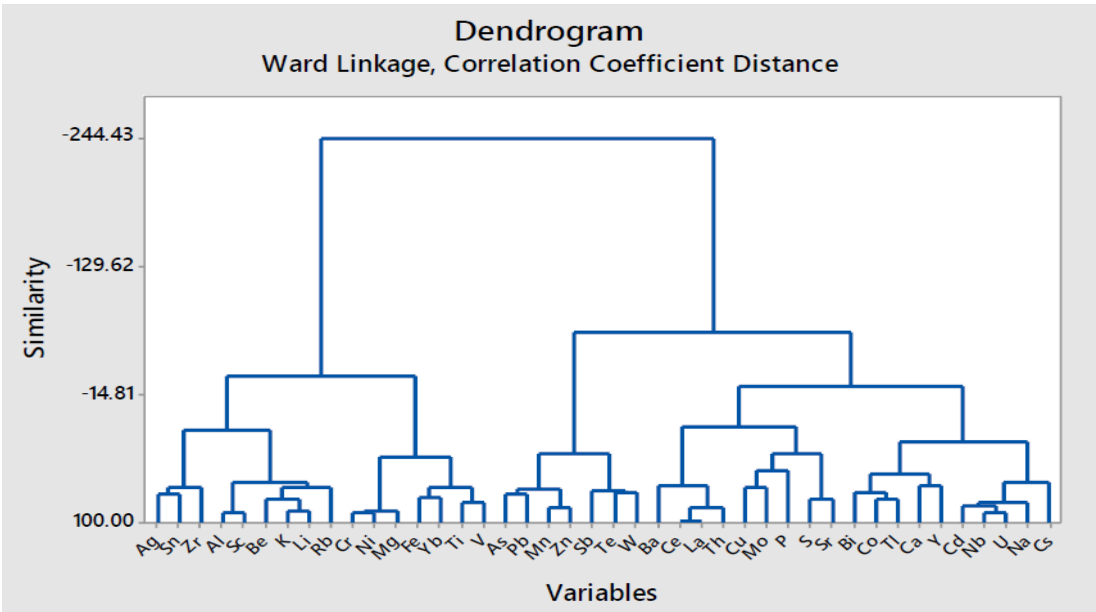

Figure 7. Result of cluster analysis of Kahang data.

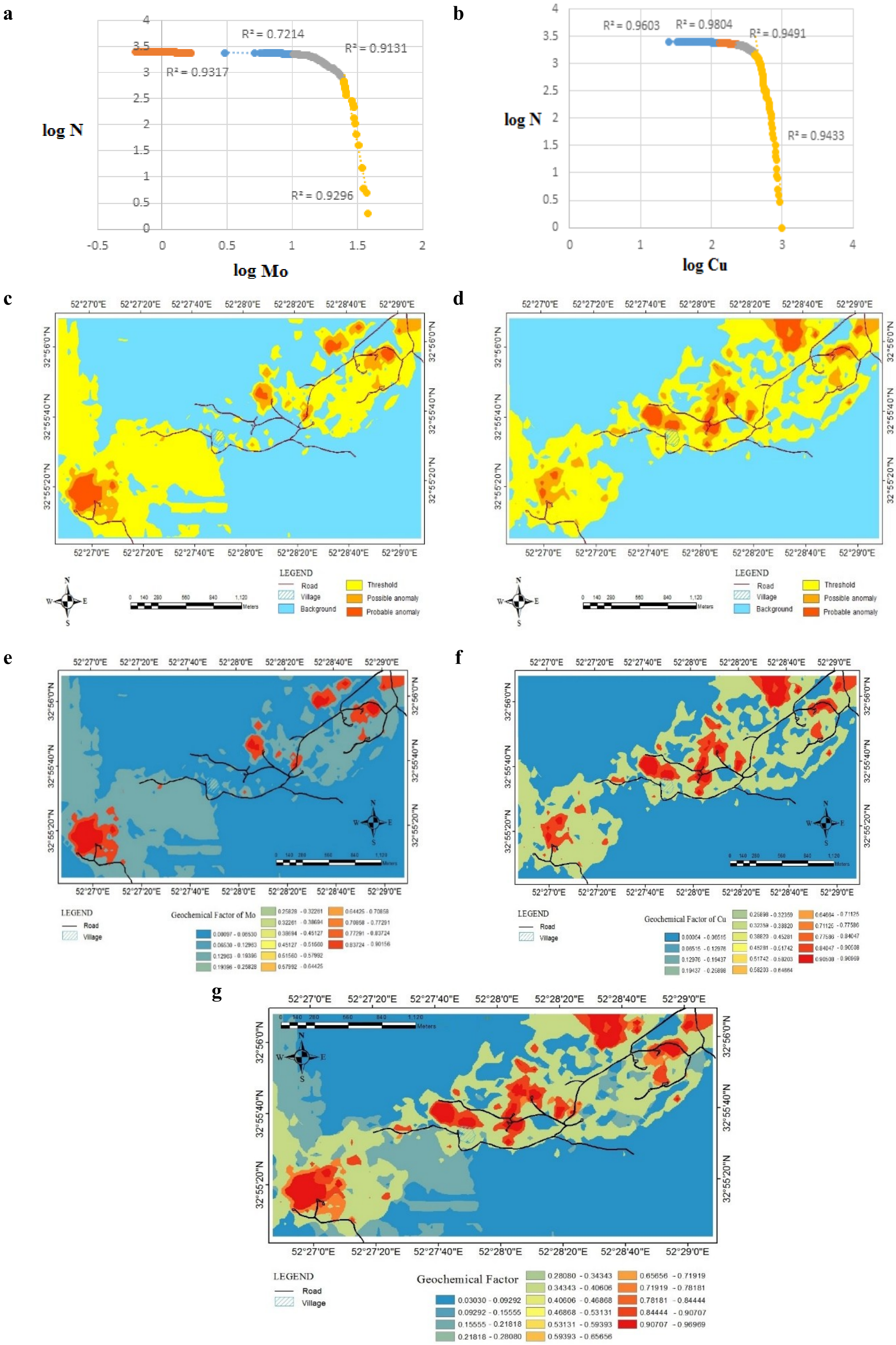

Figure 8. (a) Logarithmic diagram of C-N for copper, and (b) for molybdenum. (c) Separation of anomaly from background by C-N fractal method for copper and (d) for molybdenum. (e) Fuzzy map of copper and (f) molybdenum. (g) Final geochemistry map of Kahang area.

Table 3. Descriptive statistics of geochemical data in Kahang area.

	Domain	Min	Max	Mean	Std. deviation	Variance
Ag	0.49	0.26	0.75	0.33	0.05	0.00
Al	90741.00	40527.00	131268.0	76016.65	13319.39	177406145.67
As	35.40	6.50	41.90	15.87	4.81	23.15
Ba	1561.00	284.00	1845.00	611.67	194.80	37946.46
Be	2.20	1.00	3.20	1.85	0.28	0.08
Bi	2.66	0.34	3.00	0.48	0.09	0.01
Ca	112956.00	7032.00	119988.0	34907.37	17106.68	292638434.97
Cd	1.95	0.23	2.18	0.37	0.23	0.06
Ce	58.00	20.00	78.00	45.36	7.05	49.74
Co	42.00	9.00	51.00	23.05	4.73	22.40
Cr	367.00	20.00	387.00	135.88	36.67	1344.51
Cs	1.94	1.30	3.24	2.05	0.24	0.06
Cu	963.00	25.00	988.00	123.97	105.62	11155.33
Fe	46486.00	21440.00	67926.00	42654.43	4930.13	24306176.30
K	44770.00	7195.00	51965.00	22270.56	5970.63	35648467.62
La	33.00	11.00	44.00	25.05	3.88	15.04
Li	47.00	10.00	57.00	34.02	6.22	38.70
Mg	19370.00	9452.00	28822.00	19694.30	2340.70	5478889.08
Mn	2701.00	264.00	2965.00	1040.92	349.95	122463.39
Mo	56.18	0.62	56.80	1.84	3.88	15.06
Na	12958.00	2998.00	15956.00	6391.88	1936.73	3750914.52
Nb	54.00	10.00	64.00	34.05	9.98	99.66
Ni	145.00	15.00	160.0	77.66	14.76	217.94
P	1892.00	486.00	2378.00	1048.68	202.45	40984.17
Pb	596.00	10.00	606.00	62.47	52.02	2705.91
Rb	103.25	43.00	146.25	82.19	13.08	170.99
S	2938.00	109.00	3047.00	529.79	358.67	128647.74
Sb	14.80	0.83	15.63	1.11	0.59	0.34
Sc	19.57	5.80	25.37	13.84	2.34	5.49
Sn	2.50	1.30	3.80	2.02	0.36	0.13
Sr	805.00	186.00	991.00	401.83	116.32	13529.84
Te	0.09	0.13	0.22	0.16	0.01	0.00
Th	12.65	4.10	16.75	8.50	1.69	2.84
Ti	12206.27	747.00	12953.27	5767.39	1452.14	2108724.74
Tl	1.20	0.20	1.40	1.07	0.10	0.01
U	2.30	1.00	3.30	2.01	0.44	0.19

6. Preparation of magnetics layer

In order to prepare the magnetics layer, data from the magnetometer was used. In this area, 4446 points were totally picked up by the PROTON MP2 MAGNETOMETER device. The dimension of the surveying grid was 20×50 m. Each point was measured three times, and the average amount was recorded. The survey area is shown in Figure 9.

The IGRF and diurnal correlations were conducted on the magnetometer data, and the total magnetic field map was obtained (Figure 10a). In fact, the intensity and the form of the anomaly depends on the lines of the magnetic survey network. These effects were successfully removed by applying different filters on the maps. The reduce to pole (RTP) technique (Figure 10b) was used on the total magnetic field map, and the result was not only caused by displacement but also regularized the final anomalies. Afterwards, the analytical signal map was created. The maximum parts of analytical signal map represent the boundary of magnetic source (Figure 10c). According to this map, the position of anomalies was discerned, which was utilized in the integrated layer.

In the stage of assigning values to the magnetics layer (analytical signal), the medium magnetic field gained the most value. It is known that the high and low levels of the magnetic property are associated with the unaltered stones and the regional sediments, respectively. Thus they do not have a significant correlation with the mineralization. The details are given in Table 1, and the final magnetics layer is shown in Figure 10d.

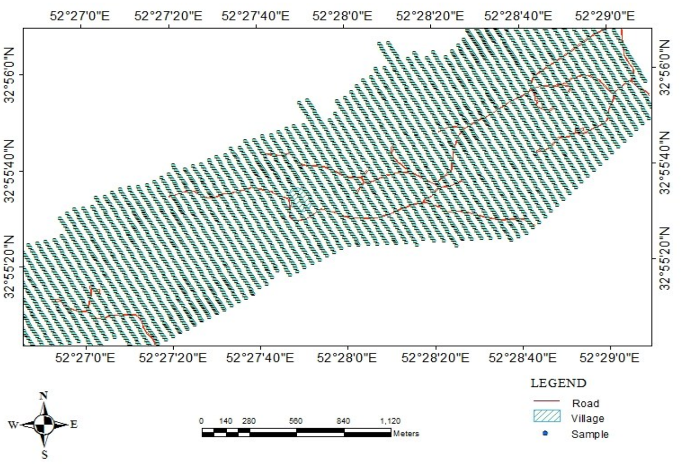

Figure 9. Location map of magnetics survey (magnetometry) in understudied area.

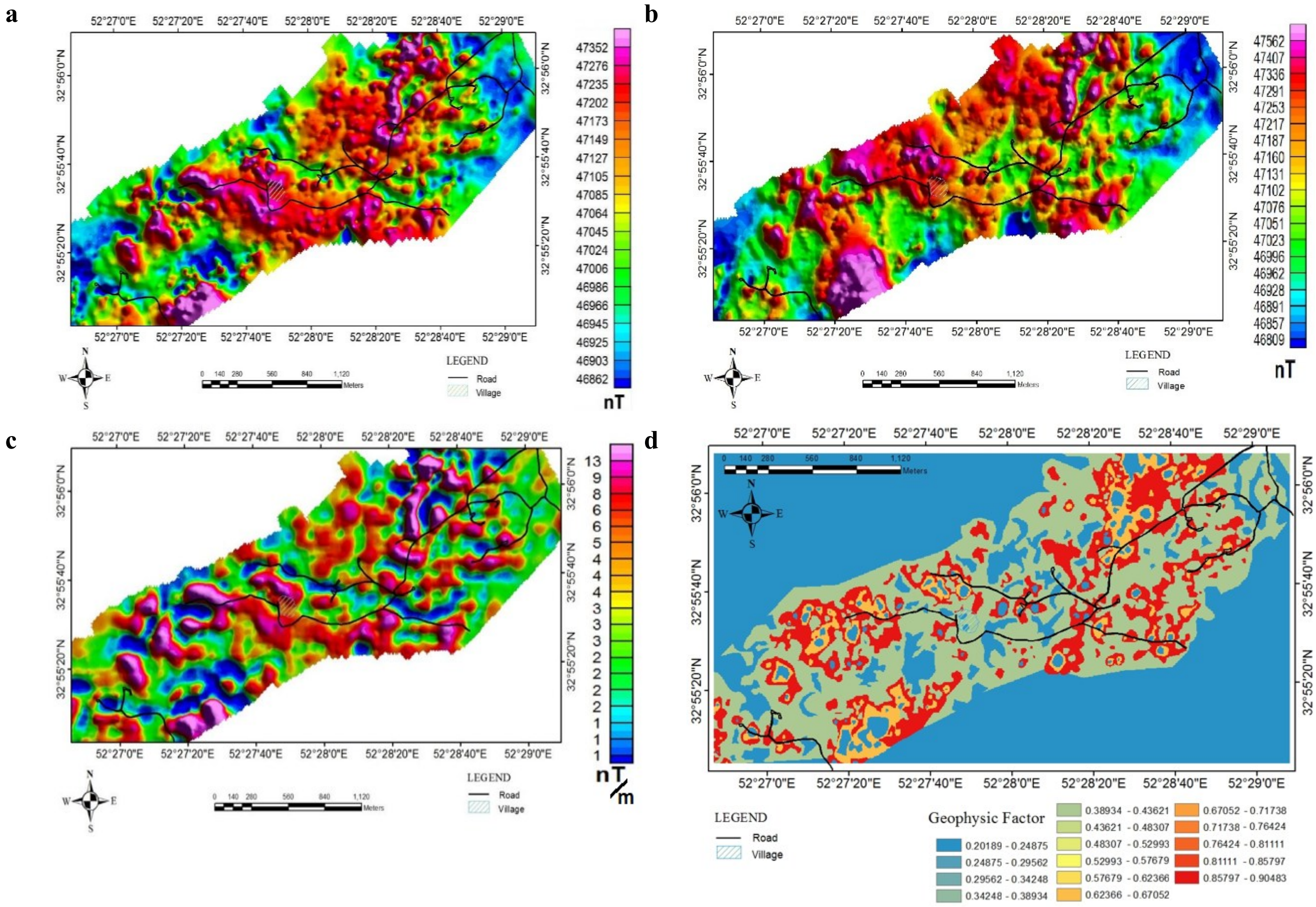

Figure 10. (a) Total magnetics field map, (b) RTP map, (c) analytical signal map, (d) final magnetics layer for understudied area.

7. Fuzzy inference system (FIS)

The fuzzy inference is a mapping technique in which the fuzzy logic applies on the inputs to provide outputs [39]. FISs can be utilized to depict an exploration geologist's logic for predicting the mineral potential by integration of predictor linguistic variables [6]. There are three inference steps in the Mamdani style including the fuzzification, inference engine, and defuzzification [7], which are illustrated in the Figure 11. All integration steps with the FIS method are briefly illustrated in Figure 12.

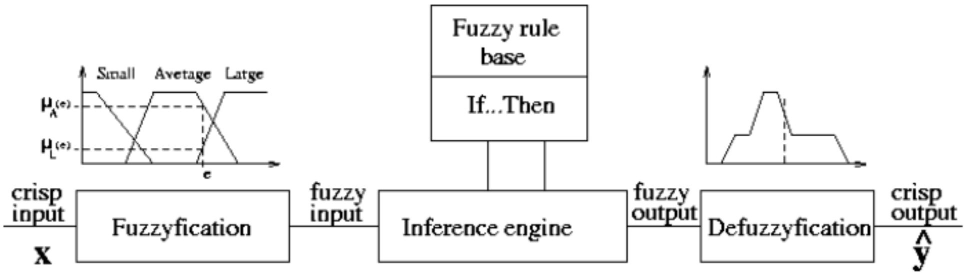

Figure 11. Modified generalized scheme for Mamdani style inference [40].

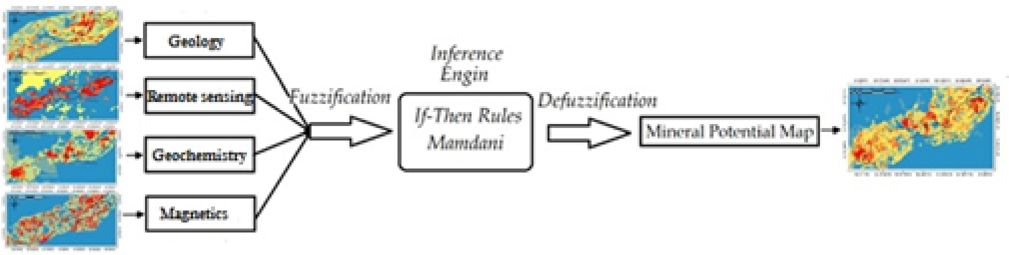

Figure 12. Schematic picture of layer integration by FIS method.

7.1. Fuzzification

Fuzzification is a kind of diagnosing membership function assigned to the fuzzy variables [41]. The various types of membership functions are triangular, trapezoidal, piecewise-linear, Gaussian, and bell-shaped. Among the mentioned types, triangular, trapezoidal, and Gaussian membership functions are only used by the geoscience researchers. The type of fuzzy membership function could greatly influence the output model. Previous studies have shown that triangle and trapezoidal functions, which are special cases of piecewise linear according to their simple nature, can be used in the green fields. However, sigmoidal/logistic and Gaussians functions, due to their nature (curvature), need at least some information about the understudied area [6, 17, 42, 43].

In this research work, the trapezoidal membership fuzzy function was applied on the input layers (i.e. geological, remote sensing, geochemical, and magnetics layers). According to the preliminary stage of exploration in the Kahang area, the trapezoidal function was used for the studied areas. Three linguistic variables including poor potential, average, and high were used to make the input maps (Figure 13a,b,c,d), while seven linguistic variables including very poor potential, poor, below average, average, and above average as well as high and very high were used to make the output map (Figure 13e).

7.2. Inference engine

In this stage, if-then rules were applied on fuzzy maps to make the final fuzzy output of the model. have shown that the number of rules (α) for layer integration is estimated by Equation (1) [44]:

$$\alpha = m^n \qquad (1)$$

where *m* is the number of language variables and *n* is the number of input variables in the FIS system (here, indicates the number of factor maps).

In order to diminish the number of rules, the layers were classified. The geology, remote sensing, geochemistry, and magnetics were the final layers to be integrated. These fuzzy layers, imported to an inference engine and 81 rules according to Eq. (1), were applied on them. Some of the rules are displayed in Table 4, and the algorithm of this process is depicted in Figure 14. It is worthy to mention to keep the figure short; the 29 of rules are only shown.

The procedure of integration of the layers in the FIS method is shown in Figure 14. According to this figure, if the pixel values are 0.495, 0.499, 0.553, and 0.500 on the geological, geochemical, magnetics, and remote sensing maps, respectively, the value for the integrated pixel will be 0.665.

7.3. Defuzzification

The final step in the FIS model is defuzzification, in which the output map of a fuzzy inference engine, i.e. a fuzzy number will be converted into a crispy number to be understandable for the mineral exploration engineers. Such a kind of

conversion is called data defuzzification. There are a variety of defuzzification models including center of gravity, weighted average, maximum mid-center, and center of the greatest levels [45]. The centroid method (Eq. 2) is the most widely used in the defuzzification step [6].
The center of gravity method, which was used in this research work, can be estimated by the following equation:

$$Z^* = \frac{\int \mu_{\bar{A}}(x)\,x\,dx}{\int \mu_{\bar{A}}(x)\,dx} \tag{2}$$

where $\mu_{\bar{A}}(x)$ is the degree of fuzzy membership for values of x that represent fuzzy membership degree in fuzzy inference output and Z* is the center of gravity for the membership function values. The value 0.665 is obtained by the center of gravity, and used to make the final mineral potential map (Figure 15).

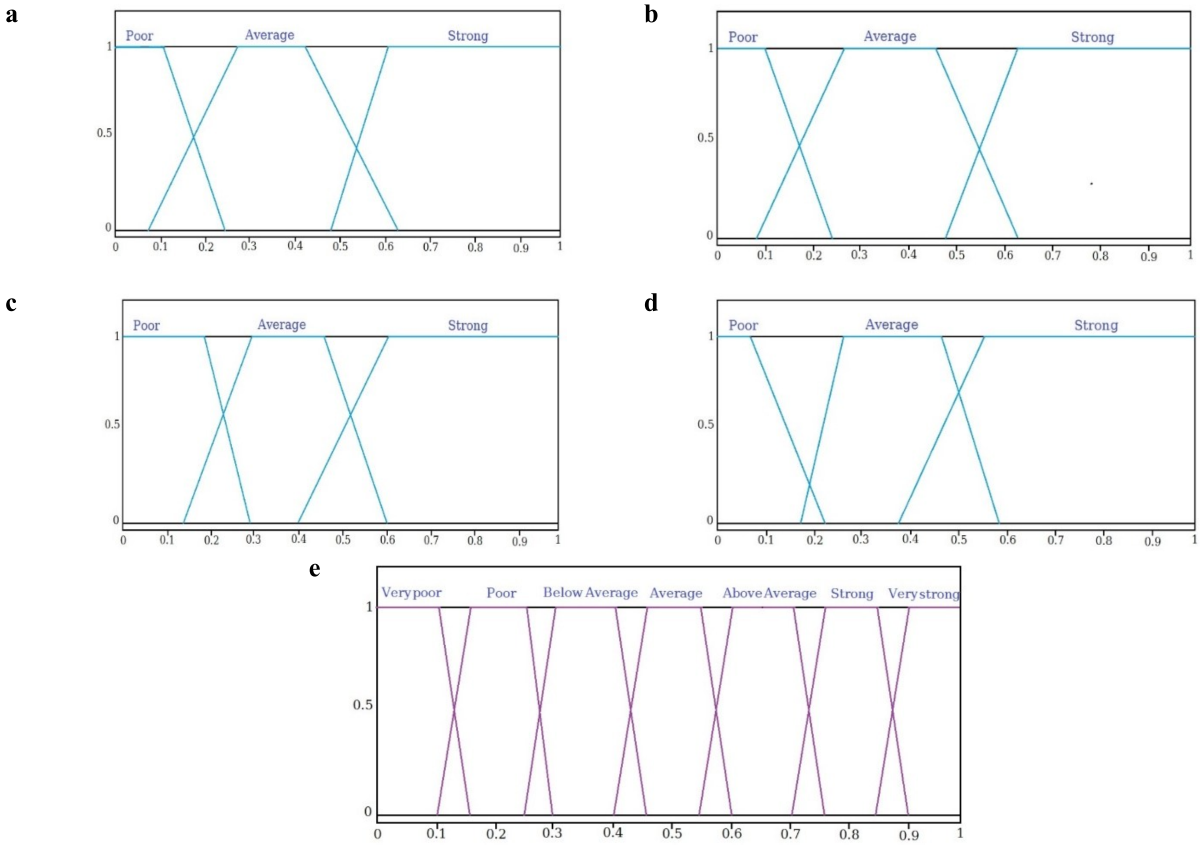

Figure 13. Membership functions, (a) geological factor, (b) remote sensing factor, (c) geochemical factor, (d) magnetics factor, (e) output factor (final mineral potential map).

Table 4. Examples of if-then rules in FIS.

Rule	Geology	Remote sensing	Geochemistry	Magnetics	Mineral potential
1	Poor	Poor	Poor	Poor	Very poor
2	Poor	Poor	Average	Poor	Poor
3	Average	Strong	Poor	Average	Average
4	Poor	Average	Strong	Strong	Above average
5	Strong	Strong	Strong	Average	Strong
6	Strong	Strong	Strong	Strong	Very strong

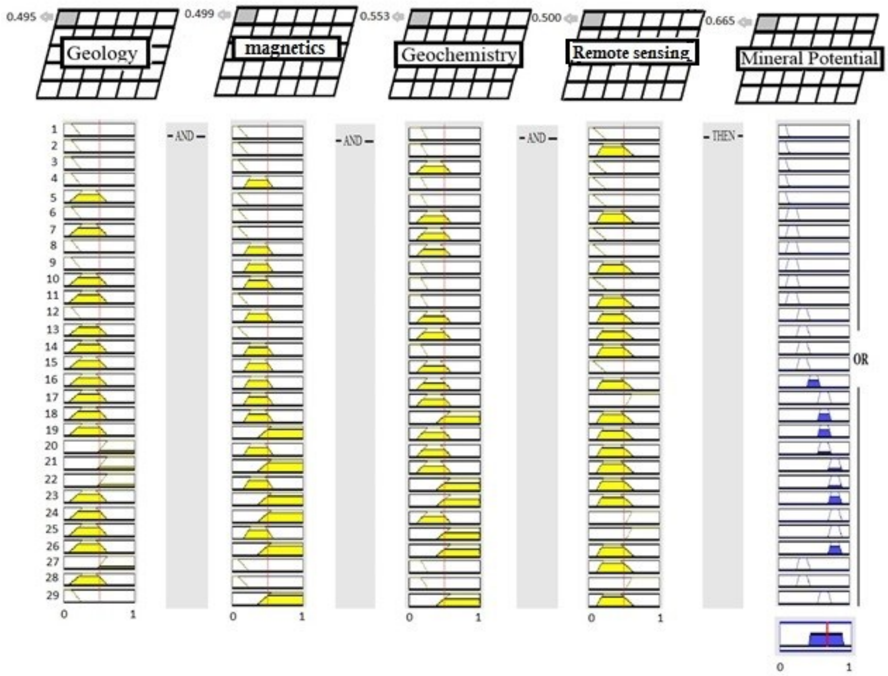

Figure 14. Procedure of integration of layers in FIS method for Kahang area.

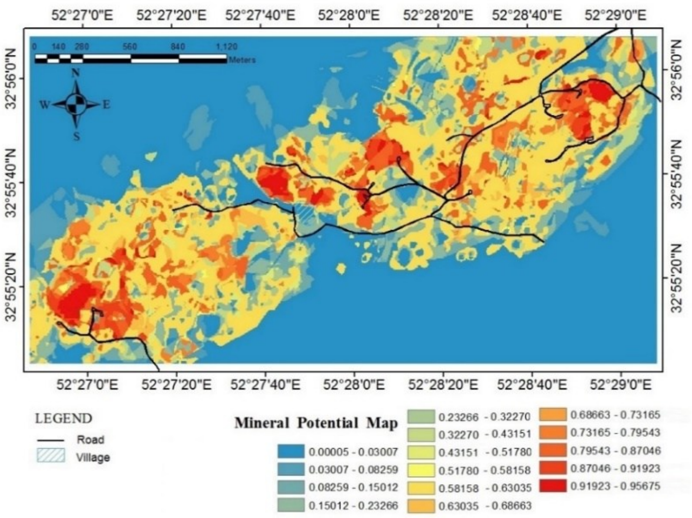

Figure 15. Final mineral potential map in Kahang area.

8. Results and discussions

8.1. Validation of results

Mineral Potential Mapping (MPM) is a multi-disciplinary task requiring the simultaneous consideration of numerous datasets including the geological, remote sensing, geochemical, and geophysical datasets. The MPM process is a multiple criteria decision making (MCDM) task, and produces a predictive model for outlining the prospective areas. Several methods exist for MCDM [46, 47]. These growing methods have been used in many scientific and industrial studies [48, 49]. Each of these modeling methods for predictive mineral potential mapping offers advantages and disadvantages, and this work endeavored simply to illustrate the possible methodology for producing a mineral prospect map using a Geographic Information System (GIS). fuzzy inference system, which is one of the well-known classical MCDM methods. The fuzzy inference technique is a widely accepted multi-attribute decision-making technique due to its sound logic, simultaneous consideration of the ideal and anti-ideal solutions, and easily programmable computation procedure. FIS, which is a type of knowledge-driven artificial intelligence systems, is transparent, easy to build, and interpretable by specialists of geology and mining because it is built in a natural language. It applies the well-established FIS algorithm to mineral potential modelling. The use of FIS in exploration of deposits is also not a new idea. This method was developed by different scientists [6, 50-52].

However, the data used in this work was selected according to relevance with respect to the porphyry copper exploration criteria. In general, the five main criteria, as the input map layers, were employed including the magnetics, geochemical, geological, and remote sensing data. Various raster-based evidential layers involving geo-datasets were integrated to prepare a mineral prospectivity mapping. We applied these multiple exploration datasets and classification of mineral prospectivity areas using the fuzzy inference techniques to delineate areas with a high potential to host mineral deposits and additional exploratory drilling targets using a GIS. Utilizing a GIS allows an expert user to rapidly evaluate the spatial geoscience data for use in mineral potential mapping projects to identify exploration targeting opportunities, as shown in Figure 16a,b. These areas may be considered suitable candidate zones for detailed studies including additional drilling targets, and the remaining area may not be favorable and should be excluded from further studies because they do not have a sufficient value to justify the detailed exploration survey. However, since the validation of the resulting mineral potential maps is a critical part of the analysis, the ability to accurately predict the locations of known Cu deposits is used to validate the mineral potential maps generated by the fuzzy inference techniques employed in this work. In the studied area, available subsurface datasets of 33 boreholes were used by multiplying the mean grade in thickness above cut off Cu¼0.2% along them. In order to evaluate the capability of the fuzzy inference technique in the context of MPM, the Jenk classification allows for the comparison of the boreholes classes. According to the Jenk classification method, the mineral potential map was firstly divided into five classes. These classes including very poor, poor, average, high, and very high were attributed to each one of the boreholes (Figure 17). According to the pixel values of the final mineral potential map, the values for boreholes were determined. Then the determined classes were compared with the situation of boreholes (Table 5). The result of this assessment showed 70.6% of agreement percentage between the model results and true data from the boreholes.

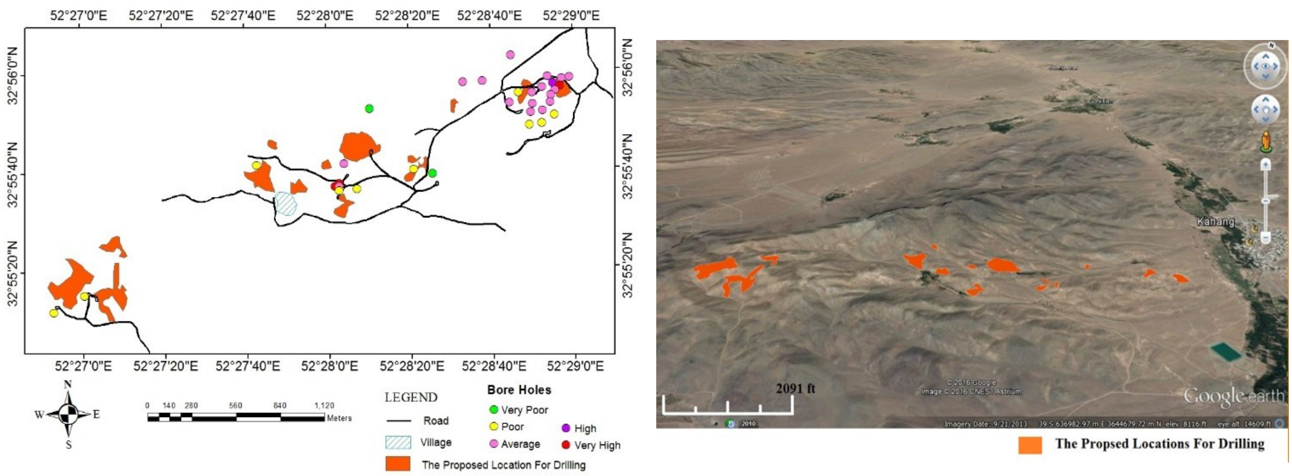

a b

Figure 16. The suggested locations for the subsequent exploration drilling.

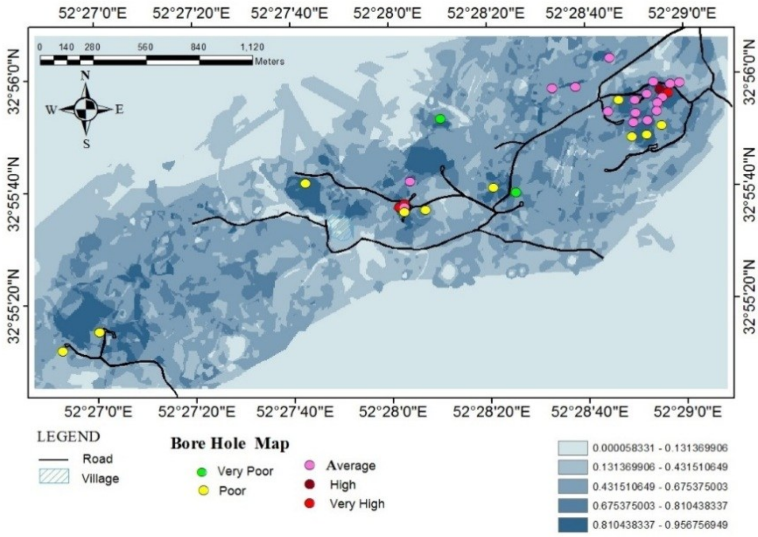

Figure 17. Agreement of drilled boreholes with final mineral potential map.

Table 5. Comparison between obtained mineral potential maps and Jenk classification method.

Number borehole	Status of borehole classified to 5 groups	Status of classification to 5 groups	Score	Number borehole	Status of borehole classified to 5 groups	Status of classification to 5 groups	Score
1	Average	Average	0	18	Average	Very high	-2
2	High	High	0	19	Poor	Average	-1
3	Very high	Very high	0	20	Very poor	Average	-2
4	Average	Average	0	21	Poor	Poor	0
5	Average	Average	0	22	Very high	Very high	0
6	Average	Very high	-2	23	Very high	Very high	0
7	Average	High	-1	24	Average	Very high	-2
8	Average	Average	0	25	Poor	Very high	-3
9	Poor	Average	-1	26	Average	Average	0
10	Poor	Very high	-3	27	Poor	High	-2
11	Average	Average	0	28	Average	Average	0
12	Poor	Average	-1	29	Poor	Average	-1
13	Average	High	-1	30	Poor	Poor	0
14	Average	High	-1	31	Average	Average	0
15	Average	High	-1	32	Very poor	Average	-2
16	Average	High	-1	33	Average	Average	0
17	Poor	Poor	0		Agreement percentage		70.6%

9. Conclusions

The target of this work was to use the fuzzy inference system to integrate layers to explore the porphyry copper deposit of the Kahang area with the lowest cost and the best result. The layers used for the process of FIS integration were geology, remote sensing, geochemical, and magnetics. The geological layer is the result of rock units and tectonic layers. The geology studies showed that there were two anomalies in the eastern and western parts of the Kahang area. In order to prepare the rock unit layer, rock units with the same grade of importance were used in the same groups, which caused to remove the effect of alluvium units and increase the effects of deeper units. Afterwards, the remote sensing studies by aster images revealed three alternations (phyllic, argillic, and propylitic) of Cu-Mo porphyry deposits in the area. The potassic alteration was detected by the lithological studies before; these four alternations prove the existence of Cu-Mo porphyry deposit in the understudied area. Since the Kahang area is hot and dry, residual soil samples were used as the geochemical data. This means that each sample refers to its location, so it makes the analysis simple. By studying multivariate statistical processes such as the Pearson correlation matrix and the cluster analysis, high correlation between copper and molybdenum elements were obtained. This statistical process with favorable rock units increases the chance of having the Cu-Mo porphyry deposit in the Kahang area. In order to separate the geochemical anomalies from background, the C-N fractal method was used, and three anomaly zones in the east, west, and central part of the area were detected. Magnetics anomalies in the understudied area were detected on volcanic rocks, andesite porphyry, and diorites, which confirmed the geological structures. Also analytical signal map demonstrated the existence of anomalies in the eastern and western parts of the area.

The results of the FIS integration system indicates that the most prospective areas for the porphyry copper mineralization in the Kahang area are located in the eastern, western, and center of Kahang. The model accuracy was validated upon achieving 70.6% agreement percentage between the final mineral potential map and true data from the 33 boreholes. In this way, the high efficiency of the FIS integrated system was confirmed as a knowledge-driven method. Therefore, the purposed FIS model could successfully suggest some locations for further exploration stages including drilling.

References

[1]. Agterberg, F.P. (1971). A probability index for detecting favourable geological environments. Canadian Institute of Mining and Metallurgy. 10: 82-91.

[2]. Agterberg, F.P. (1973). Probabilistic models to evaluate regional mineral potential. In Mathematical methods in geoscience. Symposium held at Pribram. Czechoslovakia. pp. 3-38.

[3]. Agterberg, F.P. (1974). Automatic contouring of geological maps to detect target areas for mineral exploration. Journal of the International Association for Mathematical Geology. 6 (4): 373-395.

[4]. Bonham-Carter, G.F., Agterberg, F.P. and Wright, D.F. (1988). Integration of geological datasets for gold exploration in Nova Scotia. Digital Geologic and Geographic Information Systems. pp. 15-23.

[5]. Brown, W., Groves, D. and Gedeon, T. (2003). Use of fuzzy membership input layers to combine subjective geological knowledge and empirical data in a neural network method for mineral-potential mapping. Natural Resources Research. 12 (3): 183-200.

[6]. Porwal, A., Das, R. D., Chaudhary, B., Gonzalez-Alvarez, I. and Kreuzer, O. (2015). Fuzzy inference systems for prospectivity modeling of mineral systems and a case-study for prospectivity mapping of surficial Uranium in Yeelirrie Area, Western Australia. Ore Geology Reviews. 71: 839-852.

[7]. Mamdani, E.H. and Assilian, S. (1975). An experiment in linguistic synthesis with a fuzzy logic controller. International journal of man-machine studies. 7 (1): 1-13.

[8]. Hunt, K.J., Haas, R. and Murray-Smith, R. (1996). Extending the functional equivalence of radial basis functionnetworks and fuzzy inference systems. IEEE Transactions on Neural Networks. 7 (3): 776-781.

[9]. Altug, S., Chen, M.Y. and Trussell, H.J. (1999). Fuzzy inference systems implemented on neural architectures for motor fault detection and diagnosis. IEEE transactions on industrial electronics. 46 (6): 1069-1079.

[10]. Ballal, M.S., Khan, Z.J., Suryawanshi, H.M. and Sonolikar, R.L. (2007). Adaptive neural fuzzy inference system for the detection of inter-turn insulation and bearing wear faults in induction motor. IEEE Transactions on Industrial Electronics. 54 (1): 250-258.

[11]. Nguyen, V.U. and Ashworth, E. (1985). Rock mass classification by fuzzy sets. In Proceedings of the 26th US symposium on rock mechanics. Rapid City. pp. 937-945.

[12]. Gokay, M.K. (1998). Fuzzy logic usage in rock mass classifications. J Chamb Min Eng Turk. 37 (4): 3-11.

[13]. Sonmez, H., Gokceoglu, C. and Ulusay, R. (2003). An application of fuzzy sets to the geological strength index (GSI) system used in rock engineering. Engineering Applications of Artificial Intelligence. 16 (3): 251-269.

[14]. Aydin, A. (2004). Fuzzy set approaches to classification of rock masses. Engineering Geology. 74 (3): 227-245.

[15]. Nefeslioglu, H.A., Gokceoglu, C. and Sonmez, H. (2006). Indirect determination of weighted joint density (wJd) by empirical and fuzzy models: Supren (Eskisehir, Turkey) marbles. Engineering Geology. 85 (3): 251-269.

[16]. Acaroglu, O., Ozdemir, L. and Asbury, B. (2008). A fuzzy logic model to predict specific energy requirement for TBM performance prediction. Tunnelling and Underground Space Technology. 23 (5): 600-608.

[17]. Osna, T., Sezer, E.A. and Akgun, A. (2014). GeoFIS: an integrated tool for the assessment of landslide susceptibility. Computers & Geosciences, 66: 20-30.

[18]. Afzal, P., Khakzad, A., Moarefvand, P., Omran, N.R., Esfandiari, B. and Alghalandis, Y.F. (2010). Geochemical anomaly separation by multifractal modeling in Kahang (Gor Gor) porphyry system, Central Iran. Journal of Geochemical Exploration. 104 (1): 34-46.

[19]. Afzal, P., Alghalandis, Y.F., Moarefvand, P., Omran, N.R. and Haroni, H.A. (2012). Application of power-spectrum–volume fractal method for detecting hypogene, supergene enrichment, leached and barren

zones in Kahang Cu porphyry deposit, Central Iran. Journal of Geochemical Exploration. 112: 131-138.

[20]. Harati, H. (2011). Investigation of geology, alteration, mineralogy and geochemistry of Kahang Cu porphyry deposit (NE of Isfahan). Islamic Azad University, Science and Research Branch, Tehran, Iran. Unpublished Ph.D. Thesis. 197 P.

[21]. Tabatabaei, S.H. and Asadi Haroni, H. (2006). Geochemical characteristics of Gor Gor Cu-Mo porphyry system. In 25th Iranian symposium on geosciences. Geological survey of Iran. Vol. 160.

[22]. Alavi, M. (1994). Tectonics of the Zagros orogenic belt of Iran: new data and interpretations. Tectonophysics. 229 (3-4): 211-238.

[23]. Berberian, F. and Berberian, M. (1981). Tectono-plutonic episodes in Iran. Zagros Hindu Kush Himalaya Geodynamic Evolution. pp. 5-32.

[24]. Stocklin, J. (1977). Structural correlation of the Alpine ranges between Iran and Central Asia. Memoire Hors-Serve. 8: 333-353.

[25]. Shahabpour, J. (1994). Post-mineralization breccia dike from the Sar Cheshmeh porphyry copper deposit, Kerman, Iran. Exploration and Mining geology. 3 (1): 39-43.

[26]. Afshooni, S.Z., Harooni, H.A. and Esmaili, D. (2011). The microthermometry study of fluid inclusions in quartz veins of Kahang deposit (north eastern of Isfahan). In 2nd National Symposium of Iranian Society of Economic Geology. Lorestan University. 144 P.

[27]. The national copper company of Iran. (2010). The report of geological and alternation studies on the western of Kahang area on the 1:1000 scale.

[28]. Mohebi, A., Mirnejad, H., Lentz, D., Behzadi, M., Dolati, A., Kani, A. and Taghizadeh, H. (2015). Controls on porphyry Cu mineralization around Hanza Mountain, south-east of Iran: An analysis of structural evolution from remote sensing, geophysical, geochemical and geological data. Ore Geology Reviews. 69: 187-198.

[29]. Pour, A.B. and Hashim, M. (2012). Identifying areas of high economic-potential copper mineralization using ASTER data in the Urumieh-Dokhtar Volcanic Belt, Iran. Advances in Space Research. 19 (1): 758-769.

[30]. Rajendran, S., Thirunavukkarasu, A., Balamurugan, G. and Shankar, K. (2011). Discrimination of iron ore deposits of granulite terrain of Southern Peninsular India using ASTER data. Journal of Asian Earth Sciences. 41 (1): 99-106.

[31]. Abrams, M.J., Brown, D., Lepley, L. and Sadowski, R. (1983). Remote sensing for porphyry copper deposits in southern Arizona. Economic Geology. 78 (4): 591-604.

[32]. Ghulam, A., Amer, R. and Kusky, T.M. (2010). Mineral exploration and alteration zone mapping in Eastern Desert of Egypt using ASTER Data. In ASPRS Annual Conference. San Diego. California. pp. 26-30.

[33]. Joseph, G. (2005). Fundamentals of remote sensing. Universities Press.

[34]. Kruse, F.A., Lefkoff, A.B., Boardman, J.W., Heidebrecht, K.B., Shapiro, A.T., Barloon, P.J. and Goetz, A.F.H. (1993). The spectral image processing system (SIPS)- interactive visualization and analysis of imaging spectrometer data. Remote sensing of environment. 44 (2-3): 145-163.

[35]. Kruse, F.A., Lefkoff, A.B., Boardman, J.W., Heidebrecht, K.B., Shapiro, A.T., Barloon, P.J. and Goetz, A.F.H. (1992). The Spectral Image Processing System (SIPS): Software for integrated analysis of AVIRIS data.

[36]. Weyermann, J., Schlapfer, D., Hueni, A., Kneubuhler, M. and Schaepman, M. (2009). Spectral angle mapper (SAM) for anisotropy class indexing in imaging spectrometry data. In Proc. SPIE. Vol. 7457.

[37]. Pan, Z., Huang, J. and Wang, F. (2013). Multi range spectral feature fitting for hyperspectral imagery in extracting oilseed rape planting area. International Journal of Applied Earth Observation and Geoinformation. 25: 21-29.

[38]. Behnia, P. (2007). Applying Mineral Mapping on Hyperspectral Data Using Spectral Feature Fitting Method Case Study: Abtorsh Area, Iran. 12th Conference of Int. Association for Mathematical Geology. pp. 477-480

[39]. Tang, X. (2004). Spatial object modelling in fuzzy topological spaces: with applications to land cover change. ITC.

[40]. Hazael, J., Brigitte, C., Didier, D. and Serge, G. (2009). Practical inference with systems of gradual implicative rules. IEEE Transactions on Fuzzy Systems. 17 (1):61-78.

[41]. Yagiz, S. and Gokceoglu, C. (2010). Application of fuzzy inference system and nonlinear regression models for predicting rock brittleness. Expert Systems with Applications. 37 (3): 2265-2272.

[42]. Shams, S., Monjezi, M., Majd, V.J. and Armaghani, D.J. (2015). Application of fuzzy inference system for prediction of rock fragmentation induced by blasting. Arabian Journal of Geosciences. 8 (12): 10819-10832.

[43]. Masters, T. (1993). Practical neural network recipes in C++. Morgan Kaufmann.

[44]. Passino, K.M., Yurkovich, S. and Reinfrank, M. (1998). Fuzzy control (Vol. 20). Menlo Park, CA: Addison-wesley.

[45]. Klir, G. and Yuan, B. (1995). Fuzzy sets and fuzzy logic (Vol. 4). New Jersey: Prentice hall.

[46]. Cheng, S., Chan, C.W. and Huang, G.H. (2002). Using multiple criteria decision analysis for supporting decisions of solid waste management. Journal of Environmental Science and Health, Part A. 37 (6): 975-990.

[47]. Opricovic, S. and Tzeng, G.H. (2004). Compromise solution by MCDM methods: A comparative analysis of VIKOR and TOPSIS. European journal of operational research. 156 (2): 445-455.

[48]. Bilsel, R.U., Büyüközkan, G. and Ruan, D. (2006). A fuzzy preference-ranking model for a quality evaluation of hospital web sites. International Journal of Intelligent Systems. 21 (11): 1181-1197.

[49]. Wang, Y.J. (2008). Applying FMCDM to evaluate financial performance of domestic airlines in Taiwan. Expert Systems with Applications. 34 (3): 1837-1845.

[50]. Duda, R.O. (1978). Development of the PROSPECTOR consultation system for mineral exploration. Final Report, SRI Projects, 5821, 6415.

[51]. Duda, R., Gaschnig, J. and Hart, P. (1979). Model design in the Prospector consultant system for mineral exploration. Expert systems in the microelectronic age. 1234: 153-167.

[52]. Alaeimoghadam, M.S., Karimi, M., Mesgari, M. and Saheb, A.N. (2014). Modeling process of mineral potential mapping using fuzzy inference system (case study: Chah Firoozeh copper deposit). Geosciences Journal. 24: 53-66.

اکتشاف کانسار مس پورفیری کهنگ با استفاده از تلفیق پیشرفته زمین‌شناسی، سنجش از دور، ژئوشیمی و داده‌های مغناطیس‌سنجی

سمانه برک*، عباس بحرودی و گلناز جوزانی کهن

دانشکده مهندسی معدن، پردیس دانشکده‌های فنی، دانشگاه تهران، ایران

ارسال ۲۰۱۷/۱/۱۲، پذیرش ۲۰۱۷/۶/۱۲

* نویسنده مسئول مکاتبات: samaneh_barak@ut.ac.ir

چکیده:

منظور از اکتشاف مواد معدنی یافتن نهشته‌های کانساری است. هدف اصلی این پژوهش استفاده از سیستم استنتاج‌گر فازی برای تلفیق لایه‌های اکتشافی که شامل زمین‌شناسی، سنجش از دور، ژئوشیمی و داده‌های مغناطیس‌سنجی است. محدوده مورد مطالعه کانسار مس پورفیری منطقه کهنگ در مرحله اکتشاف مقدماتی است. برای تهیه لایه زمین‌شناسی لایه‌های تکتونیکی و واحدهای سنگی با یکدیگر تلفیق شدند. برای بارزسازی دگرسانی‌ها تصاویر سنجنده استر مورد استفاده قرار گرفت و برای تهیه لایه دگرسانی انواع پردازش‌های تصویر پایه شامل ترکیب رنگی کاذب، نسبت‌های باندی و آنالیز مؤلفه‌های اصلی و همچنین طیف پایه شامل نقشه‌برداری زاویه طیفی و تطبیق ویژگی‌های طیفی بر روی تصاویر استر انجام گرفت. برای تهیه لایه ژئوشیمیایی پردازش‌های آماری چند متغیره از قبیل ماتریس همبستگی پیرسون و دندوگرام بر روی داده‌ها انجام گرفت که در نتیجه آن دو عنصر مس و مولیبدن تأثیرگذارترین عناصر کانی‌سازی شناخته شدند. برای جداسازی آنومالی از زمینه از روش فرکتال عیار- تعداد استفاده شد و در نهایت با تلفیق دو لایه مس و مولیبدن لایه ژئوشیمیایی به دست آمد. برای تهیه لایه ژئوفیزیکی داده‌های مغناطیس‌سنجی استفاده شد و نقشه سیگنال تحلیلی به عنوان لایه ژئوفیزیکی انتخاب شد. در نهایت نقشه پتانسیل معدنی منطقه پس از تلفیق لایه‌ها به وسیله سیستم استنتاج‌گر فازی به دست آمد. نقشه نهایی منطقه جهت اعتبارسنجی با اطلاعات ۳۳ حلقه گمانه حفاری شده در منطقه مقایسه شد که گویای ۷۰/۶٪ انطباق است و در نتیجه مناطقی برای حفاری‌های بعدی پیشنهاد شدند.

کلمات کلیدی: سیستم استنتاج‌گر فازی، سیستم اطلاعات جغرافیایی، نقشه پتانسیل معدنی، کهنگ، پورفیری.